

The Infrared Spectrum of H<sub>2</sub>S from 1 to 5 μm

Alexander D. Bykov, Olga V. Naumenko, Maxim A. Smirnov, Leonid N. Sinita

Institute of Atmospheric Optics

S11, Russian Academy of Science, Tomsk, Russia

Linda R. Brown, Joy Crisp and David Crisp

Jet Propulsion Laboratory, California Institute of Technology,

Pasadena, CA 91109, USA

Manuscript pages .7

Tables: .6

Figures: .2

send revisions and galley proofs to:

Dr. Linda R. Brown  
Jet Propulsion Laboratory, mail stop 183-301  
California Institute of Technology  
Pasadena, Ca 91109

## Abstract

The absorption spectra of  $\text{H}_2\text{S}$  from 2000 to  $11,147\text{ cm}^{-1}$  have been obtained with spectral resolutions of 0.006, 0.012 and  $0.021\text{ cm}^{-1}$  using the Fourier transform spectrometer at Kitt Peak National Observatory. The transitions of 20 bands have been assigned for the first time and 8 others re-analyzed so that accurate energy levels, band origins and rotational parameters could be determined. The analysis of these data revealed some remarkable features in the energy spectrum, e.g. fourfold clustering of rotational levels belonging to the symmetric and asymmetric components of local mode manifolds at a high degree of stretching excitation. This paper reports fitted vibrational parameters and predicted band origins of  $\text{H}_2\text{S}$  up to  $12,735\text{ cm}^{-1}$ . It also presents the degenerate rotational constants and upper state energies of (301)-(202) and (311)-(2,12.) at  $1\text{ }\mu\text{m}$  as illustrations of clustering in the local mode limit.

## 1. introduction

The detailed knowledge of hydrogen sulfide absorption spectra has application for terrestrial atmospheric pollutant measurements and for the investigation of chemistry in the Jovian atmosphere. From a theoretical viewpoint, hydrogen sulfide is an interesting example of a light asymmetric rotor for which the internal nuclear motion can be strongly perturbed by intramolecular interactions arising from vibrational or rotational excitation. For this reason, the vibrational-rotational energy spectrum of  $\text{H}_2\text{S}$  has been modeled in numerous papers using new theoretical approaches to demonstrate the effects of the local mode vibrations or bending-rotation coupling [1-3]. The infrared spectrum of  $\text{H}_2\text{S}$  has been the subject of several high resolution studies concerning the ground vibrational state [4,5], the first excited level (010) at  $8.3\text{ }\mu\text{m}$  [6,7], the first triad of interacting states {(020)-(100)-(001)} at  $4\text{ }\mu\text{m}$  [8], two levels {(110)-(011)} from the second triad at  $2.7\text{ }\mu\text{m}$  [9] and the {(101)-(200)} [10] and {(111)-(210)} [11] states belonging to the first and second hexade at  $2\text{ }\mu\text{m}$  and  $1.6\text{ }\mu\text{m}$ , respectively. However, up to now, the knowledge of hydrogen sulfide absorption and its energy spectrum has been incomplete, especially in the case of weak overtone stretching and bending modes. The lack of experimental data has limited both the theoretical analysis and the prediction of the near-infrared and the visible regions.

The present study reports the vibrational assignment of  $\text{H}_2\text{S}$  over a wide spectral interval from 2000 to  $11,147\text{ cm}^{-1}$ . In all, transitions of a total of 29 vibrational bands have been observed. Of these, 20 bands, including (311) at  $11008\text{ cm}^{-1}$ , have been identified at high resolution for the first time. In this report, we present the vibrational energy levels analysis along with the rotational assignments of pairs of parallel and perpendicular bands at  $1\text{ }\mu\text{m}$  which become rotationally degenerate in the local mode limit.

## 2. Experimental details

Laboratory spectra of  $\text{H}_2\text{S}$  were recorded at 0.006, 0.012, and 0.020  $\text{cm}^{-1}$  resolution with the Fourier transform spectrometer located at the McMath telescope facility at Kitt Peak National Observatory/ National Solar Observatory. Data were obtained using three different beamsplitters (KCl,  $\text{CaF}_2$  and quartz) in conjunction with As-doped silicon, InSb and photo-diode detectors in five different band pass intervals: 1000-2600  $\text{cm}^{-1}$ , 1800-5500  $\text{cm}^{-1}$ , 3600-8000  $\text{cm}^{-1}$ , 3600- 10,000  $\text{cm}^{-1}$  and 8600- 16,000  $\text{cm}^{-1}$ . The optical sources were a globar at longer wavelengths and a quartz projection lamp in the near-infrared and visible regions. Optical path lengths were changed from 1.5 m to a maximum of 433 m by using 3 different stainless steel absorption cells. Sample pressures were varied from 1.49 to 30 torr at room temperature. A second absorption cell containing CO was generally in series with the  $\text{H}_2\text{S}$  cell to establish the frequency calibration in the near-infrared using the 2-0 positions reported by Pollock et al. [12]. Each spectrum was usually integrated 70 to 80 minutes to produce signal to noise ratios ranging from 1000:1 at 2.5  $\mu\text{m}$  to 400:1 at 8  $\mu\text{m}$  to 50:1 at 1  $\mu\text{m}$ . Figure 1 is given as an example of the spectrum in the P branch of (021) recorded at 0.012  $\text{cm}^{-1}$  resolution with a 28 m optical path and 9.99 torr of  $\text{H}_2\text{S}$  at 289.3 K.

The line centers were determined either by doing first and second derivatives of the apodized spectra or by least-square fitting of the Voigt contour with the unapodized data. The precision and accuracy of a line center varied according to the region, gas pressure and degree of blending with other features. At 4  $\mu\text{m}$  where the resolution was 0.012  $\text{cm}^{-1}$ , the precision is 0.0001  $\text{cm}^{-1}$  for isolated lines. However, at 11,000  $\text{cm}^{-1}$  where the resolution was 0.021  $\text{cm}^{-1}$ , the precision at best is 0.0010  $\text{cm}^{-1}$  because the signal to noise was much worse. In addition, higher sample pressures of 10 to 30 torr were required to observe these very weak bands so that line centers are affected by pressure shifts. The absolute line positions were further degraded because no suitable calibration lines were available near 1  $\mu\text{m}$ ; for the interim, these data are calibrated using  $\text{H}_2\text{S}$  lines at 8800  $\text{cm}^{-1}$  recorded using the 3600 to 10,000  $\text{cm}^{-1}$  band pass with the same gas sample.

## 3. Line assignments and rotational energy levels

The line assignments were made using the combination differences and estimated line frequencies and strengths as described in Ref.[13]. The line assignment process was followed by continual fitting of the rotational constants to obtain better predicted line positions and relative strengths. Such a procedure often permitted the identification of weak lines which could not be assigned by usual combination difference methods. Figure 2 summarizes the upper vibrational states of 24 bands belonging to different interacting band systems (triad, hexad, decade and quindecade) that have been observed so far in the near-infrared portion of the Kitt Peak spectra. The extent of identification is given by indicating the largest values of the J and  $K_a$  quantum numbers [ $J_{\text{max}}$  and  $K_{a\text{max}}$ ] obtained up to now and the total number of upper state levels assigned. New band origins were obtained either using the observed assignment of P(1,1,1) or 1'(1,0,1) to the 0,0,0 levels or by fitting all available assignments.

#### 4. The vibrational energy levels of H<sub>2</sub><sup>32</sup>S

The two previous [7,8] and 28 new band origins have been combined to determine the effective vibrational Hamiltonian constants and to calculate the highly excited vibrational levels. The effective vibrational Hamiltonian is the "spectroscopic Hamiltonian" of Ref.[14] that includes the high anharmonic terms:

$$H = \sum_{ij} H_{ij} |i\rangle \langle j|$$

$$H_{ii} = \sum_{\lambda} \omega_{\lambda} \left( v_{\lambda}^i + \frac{1}{2} \right) + \sum_{\lambda, \mu > \lambda} X_{\lambda\mu} \left( v_{\lambda}^i + \frac{1}{2} \right) \left( v_{\mu}^i + \frac{1}{2} \right) + \sum_{\lambda, \mu > \lambda, \nu > \mu} Y_{\lambda\mu\nu} \left( v_{\lambda}^i + \frac{1}{2} \right) \left( v_{\mu}^i + \frac{1}{2} \right) \left( v_{\nu}^i + \frac{1}{2} \right) + \dots$$

$$H_{ij} = \left\{ \Gamma_{DD} + \gamma_1 \left( v_1 + \frac{1}{2} \pm 2 \right) + \gamma_2 \left( v_2 + \frac{1}{2} \right) + \gamma_3 \left( v_3 + \frac{1}{2} \mp 2 \right) \right\} \\ \times \left\{ \left( v_1 + \frac{1}{2} \pm \frac{1}{2} \right) \left( v_1 + \frac{1}{2} \pm \frac{3}{2} \right) \left( v_3 + \frac{1}{2} \mp \frac{3}{2} \right) \left( v_3 + \frac{1}{2} \mp \frac{1}{2} \right) \right\}^{1/2}$$

if

$$|i\rangle = |v_1 v_2 v_3\rangle, \quad |j\rangle = |v_1 \pm 2 v_2 v_3 \mp 2\rangle \quad (\text{Darling-Dennison resonance}).$$

The spectroscopic parameters determined are the harmonic frequencies  $\omega_1, \omega_2$  and  $\omega_3$ , anharmonic  $X_{ij}, Y_{ijk}$  constants and the coupling Darling-Dennison resonance constants  $\Gamma_{DD}$  and  $\gamma_2$ . The Fermi-resonance has not been included in the calculations because it has been found to be insignificant. The fitted vibrational parameters of hydrogen sulfide are shown in Table 1 together with estimated uncertainties (one standard deviation). The calculated vibrational energy levels of H<sub>2</sub>S up to 13000 cm<sup>-1</sup> and the available experimental values are presented in the second and third columns of Table 2. It may be seen that all the fitted constants are well-determined. The maximum difference between observed and calculated vibrational energy levels is equal to 0.07 cm<sup>-1</sup>, and the standard deviation is 0.037 cm<sup>-1</sup> for 30 observed band centers. Although the fit does not reproduce the band centers to their experimental accuracies, it has to be emphasized that this vibrational energy levels calculation is the best in the literature to date. We believe that reproduction of the experimental data at this level does provide a useful prediction of the highly excited states.

The results of the "ab initio" calculation [15] of the vibrational constants and levels (column 6, Table 2) seem to be in qualitative agreement with our data. We do note that there are some large differences between the experimental values and the "ab initio"

calculations for the (040) state and other higher vibrational states involving the bending vibration. The levels involving low excitation of the bending mode ( $v_2 < 3$ ) calculated by Kozin and Jensen [3] using the variational MORBID (Morse Oscillator Rigid Bender Internal Dynamics) method (column 5, Table 2) agree within  $1 \text{ cm}^{-1}$  with our results. For states involving the excited bending vibration, the differences between our and the Kozin, Jensen calculations range from  $2 \text{ cm}^{-1}$  for (040) state to  $30 \text{ cm}^{-1}$  for highest bending state (080). Note that in the case of our calculations, the agreement for the (040) state is satisfactory because its observed upper state level was used in our fitting, while in the Kozin, Jensen paper the (040) energy value is purely a prediction.

The MORBID approach uses the exact vibration-rotation Hamiltonian with the intramolecular potential energy function having a reasonable asymptotic behavior. Energy levels are calculated by a "direct" numerical diagonalization, and the potential energy function parameters are fitted to a large number of rotational-vibrational levels of four isotopic species of hydrogen sulfide. The MORBID calculations have to give accurate energy levels; hence the good agreement between our levels and those predicted within the MORBID approach is evidence of the validity of the effective vibrational Hamiltonian method.

## 5. The local modes in hydrogen sulfide

### S.1 Vibrational energy spectrum of $\text{H}_2\text{S}$ and local mode limit.

The traditional theory of vibrational-rotational spectra is based on the concept of normal coordinates and a perturbation treatment of vibration-rotation interactions with anharmonic corrections and relevant effective rotational Hamiltonians [16]. The conventional approach has been successful in explaining the spectra caused by transitions to low-lying vibrational states, but other approaches are required for highly excited vibrational states. The local mode model has been successfully applied to fit the vibrational spectra of  $\text{H}_2\text{X}$ ,  $\text{XH}_3$ ,  $\text{XH}_4$  and several other types of molecules (see for instance [17-27]). In this treatment, the molecule is represented as the sum of independent Morse-oscillators with a weak potential and kinetic couplings between them while the bending vibration is frozen. The local mode model does explain the spacing between states of symmetric and asymmetric vibrational mode (the local mode pair) and the degeneracy of these levels under high excitation.

A extensive set of  $\text{H}_2\text{S}$  vibrational-rotation energies (experimental and calculated) gives us an unique opportunity to understand the local mode limit in some detail. We first note that the relation predicted by Mills and Robiette [Eq. 24 of Ref. 26] is satisfied by the fitted  $\text{H}_2\text{S}$  parameters shown in Table 1.

$$x_{11} = x_{33} = 0.25 \quad x_{13} = \Gamma_{\text{DB}} \quad \text{or} \quad -24.3 \approx -24.5 \approx -23.7 \approx -23.3$$

Secondly, we can determine the energy where the local mode limit is reached so that the stretching modes become degenerate. The energy differences between stretching pairs ( $\text{H}_{\text{B1}} -$

$1 \nu_{A1}$ ) are presented in Table 3. When bending vibration is frozen (column 1 in the Table 3) the stretching pairs become degenerate beginning at  $n=3$ . When the number of the stretching quanta are small, the increase of the bending vibration quanta leads to a sharp decrease of  $E_{B1}-E_{A1}$ . When the number of the stretching quanta exceeds 2, the bending vibration does not affect the degeneracy of the pairs.

## 5.2 Rotational energy levels at the local mode limit

Despite extensive studies of local mode vibrational motion in different types of molecules, there is only limited information about the rotation-vibration energy structure for the case of local mode behavior (see Ref. 25). Existing models employ simplifying assumptions about the intra-molecular potential energy function [23]. Little has been reported about the rotational structure in the local mode limit.

In the present study, we have examined the rotation-vibration energy levels of the nearly degenerate pairs of vibrational states corresponding to the excitation of three and four quanta of the stretching vibration. Band origins and rotational constants have been determined by fitting experimental energy levels. For example, the calculated and observed upper state levels, the differences between observed and calculated values, and the mixing coefficients for the  $\{(301)-(202)\}$  and  $\{(311)-(212)\}$  local mode pairs are presented in Tables 4 and 5, respectively. We noted some interesting features. First, all levels of the stretching pairs are at least doubly degenerate, despite the fact that they are determined from different sets of lines of parallel and perpendicular bands. In first pair, the degenerate pairs consist of one level belonging to (301) and another one belonging to (202). The degeneracy is within  $0.018 \text{ cm}^{-1}$  for levels listed in Table 4.

To model the observed levels, the effective rotational Hamiltonian is written in the usual manner; apart from Watson-type "diagonal" Hamiltonian, it contains the Coriolis-type "resonance" operator. If we use the Hamiltonian with different rotational and centrifugal distortion constants for the two vibrational states belonging to the given local mode pair, we find that the parameters of two states are very similar. For instance, the rotational constants of the (301) and (202) pair are  $9.61598 \pm 0.00060$ ,  $8.61483 \pm 0.00071$ ,  $4.47645 \pm 0.00013$  and  $9.61589 \pm 0.00069$ ,  $8.61315 \pm 0.00077$ ,  $4.47677 \pm 0.00017$  for A, B and C constants, respectively, and the centrifugal distortion constants are equally close. If we force the rotational constants of the pairs to be equal, reducing the number of fitted parameters from 17 to 9, the quality of the fitting does not change very much; in the first case, the standard deviation is  $0.005 \text{ cm}^{-1}$  and for the second it is  $0.006 \text{ cm}^{-1}$ . Thus, one can conclude that the highly excited local mode vibrations lead to an alignment of rotational and centrifugal distortion constants for the paired states and that the parameters become identical. As a consequence one can use for the calculations the simple models with fewer adjustable parameters. The fitted parameters for these states are presented in Table 6. The Hamiltonian reproduces the experimental data well enough to assign unambiguously the spectrum recorded at  $0.02 \text{ cm}^{-1}$  resolution. For 120 energy levels of (301)-(202) and 129 levels of (311)-(212), the standard deviations are  $0.006 \text{ cm}^{-1}$ , and the largest deviation is  $0.017 \text{ cm}^{-1}$ .

As it is seen from Tables 4 and 5, the mixing between rotational sublevels is strong. There are numerous levels with approximately fifty-fifty mixing, and the maximum of the mixing shifts toward the larger values of the  $K_a$  quantum number with increasing  $J$ . This causes the strengthening of the weak component of local mode pair (e.g. (202)). As a consequence, there are a large number of lines which are actually doublets. This leads to some difficulties in the energy levels determination. We have also found examples of fourfold clustering in the (301)-(202) pair starting with  $J=4$  levels at  $K_a=0$  and 1 of both states. For  $J=6$ , the degeneracy is  $0.001\text{ cm}^{-1}$ , and analogous clustering takes place for  $K_a=1$  and 2 levels starting at  $J=6$ , and for  $K_a=2$  and 3 at  $J=8$  etc. This kind of fourfold clustering was previously predicted by Lehmann [23] and later was confirmed by Kozin and Jensen during MORBID calculations for  $\nu_1/\nu_3$  bands of  $\text{H}_2\text{S}$  [3] and  $\text{H}_2\text{Se}$  [27]. This type of clustering is formed by "coexistence" of two energy doublets belonging to states of local mode pair. The present result is experimental evidence of this phenomena at low  $J$  and  $K_a$  values,

### Conclusion

The large set of rotational-vibration energy levels obtained from the high resolution Fourier-Transform spectra of  $\text{H}_2\text{S}$  up to  $11,147\text{ cm}^{-1}$  has permitted detailed studies of its vibrational structure in the local mode limit. The high excited bending vibrational states (030), (040), (130) and (031) have been analyzed for the first time so that the bending-vibrational interactions could be investigated. The local mode limit is clearly demonstrated in several highly excited vibrational states: (211)-(112), (301)-(202), and (311)-(212). The rotational structure of the stretching pairs is completely degenerate from  $J=0$  up to  $J=10$ , and the spacing between corresponding levels in the stretching pairs is less than  $0.02\text{ cm}^{-1}$ . This allows the mixing of the spectroscopic parameters of one vibrational component with another component of the stretching pair. As a result, a fourfold degeneracy of the  $K_a=0$  and  $K_a=1$  arises at low  $J$ -values when strong excitation of the local modes occurs.

### Acknowledgements

The authors thank the Kitt Peak National Observatory/National Solar Observatory for the use of the FTS and C. Plymate and J. Wagner for assistance in obtaining the  $\text{H}_2\text{S}$  spectra. We also thank Kozin and Jensen for making results available to us prior to publication. Part of the research reported in this paper was performed at the Jet Propulsion Laboratory, California Institute of Technology, under contract with the National Aeronautics and Space Administration.

## References

1. S. Miller, J. Tennyson, P. Rosmus, J. Senekowitsch, and I. M. Mills, *J. Mol. Spectrosc.* **143**, 61 (1990).
2. J. Makarewicz, and J. Pyka, *Mol. Phys.* **68**, 107 (1989).
3. I. N. Kozin, and P. Jensen, *J. Mol. Spectrosc.* **163**, 483 (1994)
4. J.-M. Flaud, C. Camy-Peyret, and J. W. C. Johns, *Can. J. Phys.* **61**, 1462, (1983).  
S. C. Camy-Peyret, J.-M. Flaud, L. Lechuga-Fossat, and J. W. C. Johns, *J. Mol. Spectrosc.* **109**, 300 (1985).
6. L. Lechuga-Fossat, *J. Mol. Spectrosc.* **97**, 9, (1983).
7. W. C. Lane, T. H. Edwards, J. R. Gillis, F. S. Bonomo, and F. J. Murcray  
*J. Mol. Spectrosc.* **111**, 320 (1985).
8. L. Lechuga-Fossat, J.-M. Flaud, C. Camy-Peyret, and J. W. C. Johns,  
*Can. J. Phys.* **62**, 1889 (1984).
9. L. E. Snyder, and T. H. Edwards, *J. Mol. Spectrosc.* **31**, 347 (1969).
10. O. V. Zotov, V. S. Makarov, O. V. Naumenko, and A. D. Bykov, *Atmospheric Optics* **4**, 798 (1991).
11. L. Lechuga-Fossat, J.-M. Flaud, C. Camy-Peyret, P. Areas, and M. Cuisenier, *Mol. Phys.* **61**, 233 (1987),
12. C. R. Pollock, F. R. Petersen, D. A. Jennings, J. S. Wells, and A. G. Maki, *J. Mol. Spectrosc.* **99**, 357 (1983).
13. P. Ormsby, B. Winnewisser, M. Winnewisser, K. Narahari Rae, A. Bykov, O. Naumenko, and L. Sinitsa, *J. Mol. Spectrosc.* ( in press )
14. T. Darling, and D. M. Dennison, *Phys. Rev.* **S7**, 128 (1940).
15. J. Senekowitsch, S. Carter, A. Zilch, I. J. Werner, and N. C. Hardy, *J. Chem. Phys.* **90**, 783 (1989).
16. D. Papoušek and M. R. Aliev, *Molecular Vibrational-Rotational Spectra*. Elsevier, Amsterdam, 1982.
17. M. S. Child, and L. Halonen, *Adv. Chem. Phys.* **S7**, 1 (1984).
18. L. Halonen, *J. Mol. Spectrosc.* **120**, 17S (1986).
19. L. Halonen, and M. S. Child, *Corn. Phys. Comm.* **51**, 173 (1988).
20. L. Halonen, and T. Barrington, Jr., *J. Chem. Phys.* **88**, 4171, (1988).
21. M. Halonen, L. Halonen, H. Burger, and P. Moritz, *J. Chem. Phys.* **95**, 7099 (1991).
22. M. Halonen, L. Halonen, H. Burger, and P. Moritz, *Chem. Phys. Lett* **203**, 157 (1993).
23. L. Halonen, and A. G. Robiette, *J. Chem. Phys.* **84**, 6861 (1986).
24. K. K. Lehmann, *J. Chem. Phys.* **95**, 2361 (1991).
25. H. Burger, and G. Graner, *J. Mol. Spectrosc.* **149**, 491 (1991).
26. I. M. Mills, and A. G. Robiette, *Mol. Phys.* **S6**, 743 (1985).
27. I. N. Kozin, and P. Jensen, *J. Mol. Spectrosc.* **161**, 186 (1993).



## FIGURES AND TABLES

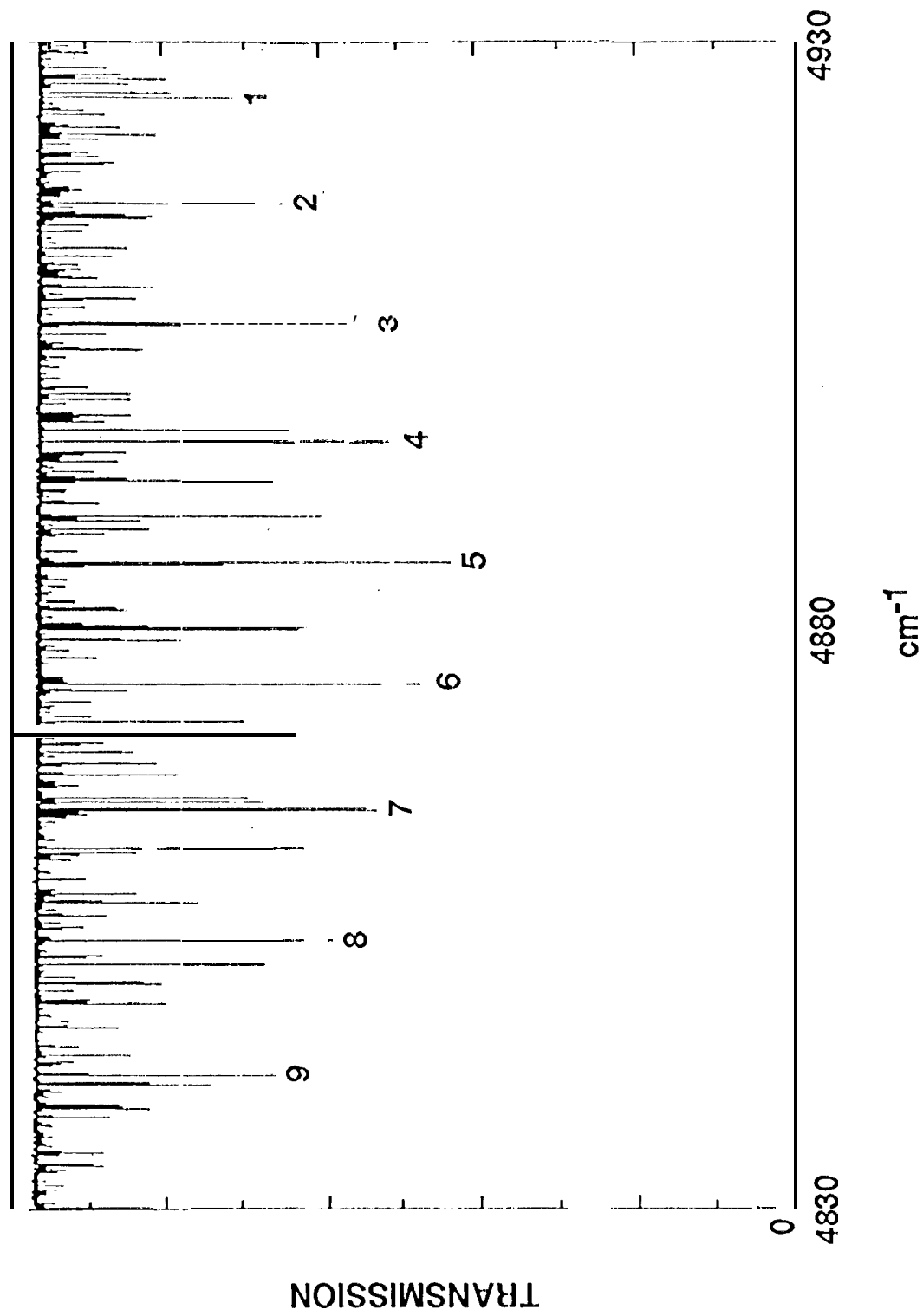
### Figures

- Figure 1. An apodized Kitt Peak FTIS spectrum of  $\text{H}_2\text{S}$  in the P branch region of (021). The  $J''$  assignment of the  $K_a = 0,1$  lines are indicated. The optical path is 28.5 m, and the sample pressure is 9.99 torr at 289.3 K.
- Figure 2. Summation of assigned levels for 24  $\text{H}_2\text{S}$  bands in the near-infrared

### Tables

- Table 1. Vibrational spectroscopic constants of  $\text{H}_2^{32}\text{S}$
- Table 2. Vibrational upper state energy levels of  $\text{H}_2^{32}\text{S}$  ( $\text{cm}^{-1}$ )
- Table 3. The energy differences in  $\text{cm}^{-1}$  between A1 and B1 stretching pairs
- Table 4. Fitted constants of  $\text{H}_2\text{S}$  (in  $\text{cm}^{-1}$ ) (301) and (202)
- Table 5. Upper state energy levels (in  $\text{cm}^{-1}$ ) and mixing coefficients for the (311) and (212) vibrational states of  $1\text{H}_2^{32}\text{S}$
- Table 6. Fitted constants (in  $\text{cm}^{-1}$ ) of local mode pairs of  $\text{H}_2\text{S}$

# TH $\approx$ P BRANCH OF $\nu_2$



J" OF STRONG k = 0, 1 PAIRS ARE INDICATED

Summation of the assigned levels for 24 H<sub>2</sub>S bands in the near-infrared

SYSTEM REGION BAND	.....SECOND TRIAD..... 2.7 $\mu$ m				.....FIRST HEXADE..... 2.0 $\mu$ m					.....SECOND HEXADE..... 1.6 $\mu$ m		
	030	110	011	040	120	021	200	101	002	130	031	121
J <sub>max</sub>	8	10	10	9	10	11	11	11	11	8	8	8
K <sub>a</sub> <sub>max</sub>	6	7	7	7	7	9	10	10	6	7	7	7
NUMBER	41	94	100	54	73	115	124	128	68	63	65	67

SYSTEM REGION BAND	.....FIRST DECADE..... 1.3 $\mu$ m				2nd DECADE 1.1 $\mu$ m			.....1st/2nd QUINDECADE..... 1 $\mu$ m				
	102	201	300	003	112	211	301	202	004	103	311	212
J <sub>max</sub>	8	8	8	8	9	9	8	8	9	9	8	7
K <sub>a</sub> <sub>max</sub>	7	8	8	8	7	8	8	7	8	8	8	7
NUMBER	75	75	75	75	74	86	74	47	58	67	63	35

SYSTEM: the total number of interacting states - triad (3), hexade (6), decade (10) and quindecade (15).  
 BAND: the quanta of  $\nu_1, \nu_2, \nu_3$ . Four of these have been previously studied at big resolution.  
 NUMBER: the total number of upper state levels assigned to maximum J and K<sub>a</sub>

Table 1. Vibrational spectroscopic constants of H<sub>2</sub><sup>32</sup>S

Parameter	Value	Parameter	Value (in cm <sup>-1</sup> )
$\omega_1$	2719.1.770(760)	$\gamma_{122} X_{100}$	- 5.82 (1.90)
$\omega_2$	1.212.840 (170)	$\gamma_{123}$	- 1.141.6 (240)
$\omega_3$	2735.8241(860)	$\gamma_{222} X_{100}$	- 6.324 (850)
$\rho_{11}$	-24.2588(120)	$\gamma_{233} X_{100}$	8.87 (200)
$x_{12}$	-17.0492(800)		
$x_{13}$	-94.9594(210)	$\rho_{DD}$	-23.27498(790)
$\rho_{22}$	-5.3160(740)	$\gamma_2$	0.4757 (120)
$x_{23}$	-21.3253(860)		
$x_{33}$	-24.4936(160)		

Estimated uncertainties in the last digits (in parentheses) are one standard deviation

Number of levels

Number of parameters 30

r s. cm<sup>-1</sup> 0.5037

Max deviation, cm<sup>-1</sup> 0.072

Table 2. Vibrational upper state energy levels of H<sub>2</sub><sup>32</sup>S (cm<sup>-1</sup>)

v <sub>1</sub>	v <sub>2</sub>	v <sub>3</sub>	E <sub>calc</sub>	E <sub>obs</sub>	o.-c*	Kozin [3] MORBID	Senekowitsch [15] ab initio
0	1	0	1182.561	1182.5742	0.014	1182.44	1190.4 [7]
0	2	0	2353.950	2353.9644	<b>0.014</b>	2353.83	2372.0
1	0	0	2614.355	2614.4080	0.052	2614.66	2620.4
0	0	1	2628.431	2628.4551	0.024	2628.56	2631.0 [8]
0	3	0	3513.789	3513.7900	0.001	3513.17	3543.5
1	1	0	3779.179	3779.1665	<b>-0.012</b>	3779.29	3794.6
0	1	1	3789.273	3789.2690	-0.004	3789.66	3799.8
0	4	0	4661.699	4661.6992	0.000	4659.48	4703.7
1	2	0	4932.715	4932.6992	<b>-0.016</b>	4932.91	4960.1
0	2	1	4939.122	4939.1045	-0.017	4939.82	4960.0
2	0	0	5145.014	5144.9858	-0.028	5145.52	5154.2
1	0	1	5147.256	5147.2207	-0.036	5147.12	5155.5
0	0	2	5243.055	5243.0016	0.046	5243.38	5251.2
0	5	0	5797.300			5791.83	5851.6
1	3	0	6074.585	6074.5825	-0.003	6074.50	6115.6
0	3	1	6077.597	6077.5952	-0.002	6078.05	6110.2
<b>2</b>	<b>1</b>	<b>0</b>	6288.160	6288.1465	-0.013	6288.37	6307.7
3	1	1	6289.220	6289.3733	<b>-0.047</b>	6288.99	6307.8
0	1	2	6386.319			6385.89	6403.0
0	<b>6</b>	<b>0</b>	6920.212			6909.29	6986.4
<b>0</b>	<b>4</b>	<b>1</b>	7204.320			7203.39	7249.4
1	4	0	7204.410			7203.10	7259.8
2	2	0	7419.818			7420.03	7451.5*
1	2	1	7420.074	7420.0908	0.017	7419.92	7452.1
<b>0</b>	<b>2</b>	<b>2</b>	7518.453			7517.74	7546.9*
<b>1</b>	<b>0</b>	<b>2</b>	7576.395	7576.3813	-0.014	7576.45*	7589.4
2	0	3	7576.555	7576.5439	-0.011	7576.42	7589.4
3	0	0	7752.288	7752.2646	-0.023	7752.40*	7768.4
0	0	3	7779.341	7779.3184	-0.023	7779.60	7789.3
0	7	0	8030.058			8010.95	8307.0
0	<b>5</b>	<b>1</b>	8318.912			8334.90	8376.5
<b>1</b>	<b>5</b>	<b>0</b>	8321.831			8317.74	8391.7
1	3	1	8539.438			8538.93	8585.9
2	3	0	8539.684			8539.53	8585.3*
0	3	2	8639.598			8637.92	8681.5*
<b>1</b>	<b>1</b>	<b>2</b>	8697.070	8697.1426	0.072	8696.58*	8723.0
2	3	1	8697.115	8697.1553	0.040	8696.48	8723.1
3	1	0	8880.066			8877.73*	8906.9
0	1	3	8899.270			8898.66	8917.4

Table 2. (continued)

$v_1$	$v_2$	$v_3$	$E_{calc}$	$E_{obs}$	$o.-c.$	Kozin [3] MORBI D	Senekowitsch [15] ab initio
0	8	0	9126.455			9095.86	
0	6	1	9420.992			9431.66	9212.7
1	6	0	9426.404			941.7.50	9490.6
1	4	1.	9646.934			9645.06	9707.9
2	4	0	9647.447			9645.95	9708.0
0	4	2	9749.111			9745.45	
2	2	1	9806.479			9805.37	9805.6
1	2	2	9806.482			9805.50*	9847.8
2	0	2	9911.008	9911.0225	0.015	991 0.77*	9848.0
3	0	3	9911.016	9911.0225	0.007	9910.75	9929.1
3	2	0	9996.658			9992.23*	
0	2	3	10008.533				
4	0	0	10188.299	10188.3008	0.002	10188.86*	
)	0	3	10194.434	10194.4482	<b>0.015</b>	10193.44	
0	0	4	10292.758				
1	5	1	10742.1.84				
2	5	0	1.0742.793				
0	5	2	10846.547				
2	3	1.	10904.285				
1	3	2	10904.297				
<b>2</b>	<b>1</b>	<b>2</b>	11008.71.3	11008.6846	-0.028		
3	1	1	11008.715	11008.6846	<b>-0.030</b>	31007.74	
3	3	0	11101.635				
0	3	3	11106.729				
4	1	0	11294.332				
1	3	3	13297.188				
0	1	4	11395.406				
<b>1</b>	<b>4</b>	<b>2</b>	33990.174				
2	4	1	11990.178				
<b>3</b>	<b>2</b>	<b>1</b>	12095.230				
2	2	2	12095.232				
3	0	2	121.49.848				
2	0	3	12149.852				
0	4	3	12193.457				
3	4	0	12194.578				
4	2	0	12388.432				
1	2	3	12389.023				
0	2	4	12488.023				
1	0	4	12524.564				
<b>4</b>	<b>0</b>	<b>1</b>	12525.150				
5	0	0	12696.428				
0	0	5	12735.256				

\* Labeling of the levels differs from that of [3] and [15]; our labeling is based on the mixing coefficients and theirs on the contribution of the basis function.

+ Energy levels for (040), (400), (202), (212) states were obtained by fitting rotational levels available with uncertainties of 0.005 cm<sup>-1</sup>.

Table 3. The energy differences in  $\text{cm}^{-1}$  between A1 and B1 stretching pairs

	$n = 1$	$E_{B1} - E_{A1}$	$n = 2$	$E_{B1} - E_{A1}$	$n = 3$	$E_{B1} - E_{A1}$	$n = 4$	$E_{B1} - E_{A1}$
$v=0$	(300, 001)	14.1	(200, 103)	2.3	(102, 201)	0.2	(202, 301)	0.0
$v=1$	(110, 011)	30.1	(230, 111)	1.3	(112, 211)	0.0	(212, 311)	0.0
$v=2$	(120, 021)	6.4	(220, 121)	0.3	(122, 221)	-0.0	(222, 321)	0.0
$v=3$	(130, 031)	3.0	(230, 131)	-0.3	(132, 231)	-0.0	(232, 331)	0.0
$v=4$	(140, 041)	-0.1	(240, 341)	-2.2	(142, 241)	-0.0	(242, 341)	0.0
$v=5$	(150, 051)	-2.9	(151, 250)	-0.6	(152, 251)	0.0	(252, 351)	0.0

$v$  is the number of bending quanta of  $\nu_2$   
 $n$  is the total number of stretching quanta of  $\nu_1$  and  $\nu_3$   
 The stretching pairs are shown in parentheses

Table 4. Upper state energy levels (in  $\text{cm}^{-1}$ ) and mixing coefficients for the (301) and (202) vibrational states of  $\text{H}_2^{32}\text{S}$

J	K <sub>a</sub>	K <sub>c</sub>	(301)				(202)					
			E <sub>calc</sub>	E <sub>obs</sub>	O-C	Mixing	E <sub>calc</sub>	E <sub>obs</sub>	O-C	Mixing		
0	0	0	9911.022	.022	0	100.0	0.0	9911.022			0.0	100.0
1	0	1	9923.854	.856	2	83.0	17.0	9923.854	.849	-4	37.0	83.0
1	1	1	9925.371	.369	-1	83.0	17.0	9925.373			17.0	83.0
1	1	0	9929.250	.253	2	100.0	0.0	9929.250			0.0	100.0
2	0	2	9947.148	.143	-5	54.4	45.6	9947.148	.141	-7	45.5	54.5
2	1	2	9946.784	.777	-6	53.4	46.6	9946.784	.781	-2	46.7	53.3
2	3	1	9958.779	.782	2	<b>82.9</b>	17.1	9958.779	.772	-6	17.1	82.9
2	2	1	9963.323	.322	0	82.9	17.1	9963.323	.315	-7	17.1	82.9
2	2	0	9966.046	.047	0	98.9	1.1	9966.046			<b>1.1</b>	98.9
3	0	3	9978.421	.421	0	86.6	13.4	9978.422			1.3.0	87.0
3	1	3	9978.364	.362	-1	86.8	13.2	9978.364			13.6	86.4
3	1	2	10001.776	.772	-3	<b>54.8</b>	45.2	10001.776	.774	-1	45.1	54.9
3	2	2	3.0000.081	.079	-1	50.4	49.6	10000.081	.087	5	49.6	50.4
3	2	1	1.0011.375	.381	5	82.2	17.8	10011.375	.370	-4	17.8	82.2
3	3	1	10020.387	.386	0	82.5	17.5	10020.387			17.6	82.4
3	3	0	10021.965	.960	-4	95.6	4.4	10021.965	.958	-6	4.4	95.6
4	0	4	10018.757	.758	0	99.4	0.6	10018.757	.752	-4	0.6	99.4
4	1	4	10018.749	.752	2	99.3	0.7	10018.749	.758	8	0.7	99*3
4	1	3	10050.634	.634	0	85.7	14.3	10050.633	.616	-16	14.3	85.7
4	2	3	10050.252	.251	0	84.2	15.8	10050.252	.245	-6	15.8	84.2
4	2	2	30074.782	.780	-1	55.5	44.5	10074.782			44.5	55.5
4	3	2	10070.300	.290	-9	45.9	54.1	10070.300	.301	0	54.1	45.9
4	3	1	30081.962	.965	2	79.8	20.2	10081.962			20.2	79.8
4	4	1	10096.656	.655	0	81.3	18.7	10096.656	.647	-8	18.7	81.3
4	4	0	10097.433	.432	0	90.4	9.6	10097.433	.423	-9	9.6	90.4
5	0	5	30068.042	.039	-2	60.2	37.8	10068.041	.040	0	46.9	53.1
5	1	5	10068.041	.040	0	<b>53.1</b>	46.9	1.0068.042	.039	-2	39.8	60.2
5	1	4	10108.901	.907	5	98.5	1.5	10108.901			1.5	98.5
5	2	4	10108.837	.835	-1	38.3	1.7	10108.836			1.7	98.3
5	2	3	3.0140.678	.672	-5	84.5	15.5	10140.678	.676	-3	15.5	84.5
5	3	3	10139.267	.266	0	79.5	20.5	10139.266			20.6	79.4
5	3	2	10166.294	.291	-2	56.7	43.3	10166.294	.294	0	43.3	56.7
5	4	2	10157.450	.444	-5	42.0	58.0	10157.451			58.0	42.0
<b>5</b>	<b>4</b>	<b>1</b>	10171.040	.036	-3	74.4	25.6	10171.040	.036	-3	25.6	74.4
5	5	1	1.0192.177	.177	0	79.4	20.6	10192.177			20.6	79.4
5	5	0	10192.518	.519	0	85.0	3.5.0	10192.517	.512	-4	15.0	85.0
6	0	6	10126.252	.250	-1	99.1	0.9	10126.252	.250	-1	47.6	52.4
6	1	6	10126.252	.250	-1.	52.4	47.6	10126.253	.250	-2	0.9	99.1
6	1	5	10176.181	.187	5	94.4	5.6	10176.1.82	.176	-5	4.4	95.6
6	2	5	10176.171	.176	4	95.6	4.4	10176.172	.187	14	5.6	94.4
6	2	4	10216.616	.620	3	96.8	3.2	10216.616			3.2	96.8
6	3	4	10216.306	.307	0	95.8	4.2	10216.306			4.2	95.8
6	3	3	10248.563	.568	4	82.8	17.2	10248.563			17.2	82.8
<b>6</b>	<b>4</b>	<b>3</b>	30244.849			<b>71.5</b>	28.5	10244.850	.833	36	28.5	71.5
6	4	2	10261.842	.837	-4	60.3	39.9	10261.843			39.9	60.1
<b>6</b>	<b>5</b>	<b>2</b>	10276.432			41.3	58.7	30276.432	.432	0	58.7	41.3
6	5	1	10279.171	.176	4	65.7	34.3	10279.173			34.3	65.7
6	6	1	10306.924	.926	1	77.0	23.0	10306.924	.920	-3	3.0	77.0
6	6	0	10307.063	.065	2	80.2	19.8	10307.062	.077	15	19.8	80.2
<b>7</b>	<b>0</b>	<b>7</b>	30193.3-76	.377	0	98.9	1.1	10193.376	.375	0	49.0	51.0



Tab] c 4 (conti nued)

J K <sub>a</sub> K <sub>c</sub>	(301)				(202)			
	E <sub>calc</sub>	E <sub>obs</sub>	O-C	Mixing	E <sub>calc</sub>	E <sub>obs</sub>	O-C	Mixing
7 1 7	10193.376	.375	0	51.0 49.0	10193.377	.377	0	1.1 98.9
7 1 6	10252.368	.363	--4	89.1 30.9	10252.369	.363	-5	5.2 94.8
7 2 6	10252.367	.363	-3	94.8 5.2	10252.367	.363	-3	10.9 89.1.
7 2 5	10301.762	.358	-3	94.3 5.9	10301.762			5.5 94.5
7 3 5	10301.703	.720	16	94.4 5.6	10301.703	.710	6	6.0 94.0
7 3 4	10341.752	.764	11	94.0 6.0	10341.751			6.0 94.0
7 4 4	10340.693	.696	2	90.8 9.2	10340.693			9.2 90.8
7 4 3	3.0374.354			80.8 19.2	10374.354			19.2 80.8
7 5 3	10366.698	.692	-5	62.2 37.8	10366.697			37.8 62.2
7 5 2	10405.282			61.3 38.7	10405.282	.297	14	38.7 61.3
7 6 2	1.0383.948	.953	4	40.5 59.5	1.0383.948			59.5 40.5
7 6 1	3.0406.679			55.4 44.6	<b>10406.678</b>			44.6 55.4
7 7 1	10440.815	.809	-6	74.2 25.8	10440.815	.808	-7	25.8 74.2
7 7 0	10440.868	.866	-1	76.0 24.0	10440.868	.865	-2	24.0 76.0
8 0 8	10269.402	.398	--3	99.7 0.3	10269.402	.398	-3	49.5 50.5
8 1 8	1.0269.402	.405	2	50.5 49.5	10269.403	.405	1	0.3 99.7
8 1 7	10337.440	.445	4	99.1 0.9	1.0337.440	.445	4	1.3 98.7
8 2 7	10337.439	.439	0	98.7 <b>1.3</b>	10337.438	.439	0	0.9 99.1
8 2 G	10395.818			86.6 13.4	10395.818			33.1 86.9
8 3 6	1.0395.808	.794	-13	86.8 13.2	10395.808	<b>.808</b>	0	13.4 86.6
8 3 5	10444.553			91.9 8.1	10444.552			8.2 91.8
8 4 5	10444.312			91.4 8.6	10444.313			8.6 91.4
8 4 4	30484.219	.200	-18	90.3 9.9	10484.217			9.9 90.1
8 5 4	1.0481.399			82.6 17.4	10481.399			17.4 82.6
8 5 3	30504.923	.929	5	46.0 54.0	10504.924			54.0 46.0
8 6 3	10553.512			53.9 46.1	10553.512			46.1 53.9
8 6 2	30552.867			64.5 35.5	10552.867			35.5 64.5
8 7 2	10524.359			44.3. 55.9	10524.360			55.9 44.1
8 7 1	3.0518.150	<b>.160</b>	9	78.7 21.3	10518.149			21.3 78.7
8 8 1	10593.728			71.2 28.8	10593.728			28.8 71.2
8 8 0	10593.746	.745	0	72.2 27.8	10593.747			27.8 72.2
9 0 9	10354.317	.316	0	55.3 44.7	10354.317	.321	3	44.3 55.7
9 1 9	10354.317	.31.6	0	55.7 44.3	10354.31.7	.321	3	44.7 55.3
9 1 8	10431.377	.385	7	98.9 1.1	10431.377	.385	7	46.3 53.7
9 2 8	10431.377	.372	-4	53.7 46.3	10431.375	.372	-2	1.1 98.9
9 2 7	10498.712			81.1 18.9	10498.711			28.4 71.6
9 3 7	10498.708	.708	0	71.6 28.4	10498.709			18.9 81.1
9 3 6	10556.341			83.2 16.8	10556.341			1.7.4 82.6
9 4 6	10556.290			82.6 17.4	10556.291			16.9 83.1
9 4 5	10604.340			88.4 11.6	10604.341			1)..6 88.4
9 5 5	10603.557			87.0 13.0	10603.558			13.0 87.0
9 5 4	10644.004			85.3 14.7	10644.005			14.7 85.3
9 6 4	10637.862			<b>71.8</b> 28.2	10637.864			28.2 71..8
9 6 3	10659.950			51.8 48.2	10659.949			48.2 51..8
9 7 3	10719.412			<b>61.4</b> 38.6	10719.412			38.6 61.4
9 7 2	10719.135			67.7 32.3	30719.334			32.3 67.7
9 8 2	10683.614			49.9 50.1	1.0683.615			50. 1. 49.9
9 8 1	10680.044			76.4 23.6	30680.045			23.6 76.4
9 9 1	10765.521			68.2 <b>31.8</b>	10765.521			31.8 68.2
9 9 0	10765.526			68.7 31.3	10765.527			31.3 68.7

O-C = observed-calculated band centers in units of 10<sup>-3</sup> cm<sup>-1</sup>

Table 5. Upper state energy levels (in cm-1) and mixing coefficients for the (311) and (212) vibrational states of H<sub>2</sub><sup>32</sup>S

J	K <sub>a</sub>	K <sub>c</sub>	(311)			(212)			O-C	Mixing	
			E <sub>calc</sub>	E <sub>obs</sub>	O-C	E <sub>calc</sub>	E <sub>obs</sub>	O-C			
0	0	0	31008.684	.684	0	100.0	0.0	11008.684		0.0	1.00.0
1	0	1	31021.667	.669	1	83.3	16.7	11021.667	.670	2	16.7 83.3
3	1	1	11023.299	.301	1	83.3	36.7	31023.299			16.7 83.3
<b>1</b>	<b>1</b>	<b>0</b>	11027.451	.451	0	100.0	0.0	11027.451	.459	7	0.0 3.00.0
2	0	2	1.1045.107	.1.07	0	54.0	46.0	11045.107	.115	7	46.1 53.9
2	1	2	31044.714	.711.	-2	52.8	47.2	11044.713	.716	2	47.1 52.9
2	1	1	11057.555	.555	0	83.3	16.7	11057.555			16.7 83.3
2	2	1	11062.443	.441	-1	83.3	1.6.7	11062.443	.440	-2	16.7 83.3
2	2	0	11065.352	.355	3	98.9	3.3.	31065.352			<b>1.1</b> 98.9
3	0	3	1.1076.331	.336	4	86.3	13.7	11076.331	.335	3	13.9 86.1
3	1	3	11076.270	.272	2	85.9	1.4.1	31076.270	.270	0	13.9 86.1.
3	1	2	11099.519	.518	0	50.1	49.9	3.1099.519	<b>.517</b>	-1	49.9 50.1
3	2	2	11101.350	.349	0	45.7	54.3	.1101.351	.356	5	54.3 45.7
<b>3</b>	<b>2</b>	<b>1</b>	3111.1.607	.604	-3	82.5	17.5	1.1111.607	.604	-3	37.5 82.5
3	3	1	11121.299	.299	0	82.8	17.2	1.1121.299	.299	0	17.2 82.8
3	3	0	1.1122.979	.980	0	95.6	4.4	1.1122.979	●979	0	4.4 9 5
4	0	4	11116.508	.510	1	99.5	0.5	3.1116.508	.506	-1	0.5 99.5
<b>4</b>	<b>1</b>	<b>4</b>	11116.500	.506	5	99.5	0.5	3.1116.500	.510	9	0.5 99.5
4	1	3	1.1150.649	.651	1	85.8	14.2	11150.649	.641	-8	14.2 85.8
4	2	3	11150.235	.232	-2	84.3	15.7	11150.234	.237	2	15.7 84.3
4	2	2	11176.514	.511	-2	55.0	45.0	11176.514			45.0 55.0
4	3	2	11171.673	.665	-7	45.5	54.5	11371.674	.672	-1	54.5 45.5
<b>4</b>	<b>3</b>	<b>1</b>	11184.167	.165	-1	80.1	19.9	11184.167	.166	0	19.9 80.1
4	4	3	11199.956	.957	0	81.6	18.4	11199.956	.955	0	3.8.4 81.6
4	4	0	11200.779	.778	0	90.5	9.5	11200.779	.783	3	9.5 90.5
5	0	5	11165.518	.524	6	96.7	3.3	11165.518	.523	5	0.9 99.1
5	1	5	11165.516	.524	8	99.1	0.9	11165.517	.524	7	3.3 96.7
5	1	4	11209.280	.286	5	98.7	1.3	11209.281			1.3 98.7
5	2	4	11209.211	.210	0	98.5	1.5	31209.211			1.5 98.5
5	2	3	11243.293	.297	3	84.6	15.4	11.243.294	.293	0	15.4 84.6
5	3	3	11241.761	.756	-4	79.5	20.5	11241.761	.753	-7	20.5 79.5
5	3	2	11270.725	.732	7	56.3	43.7	11270.726	.721	-4	43.7 56.3
5	4	2	11261.189	.181	-8	41.7	58.3	11261..190			58.3 41.7
5	4	1	11275.769	.775	6	74.7	25.3	11275.767	.765	-1	25.3 74.7
<b>5</b>	<b>5</b>	<b>1</b>	11298.449	.449	0	79.8	20.2	11298.449	.449	0	20.2 79.8
5	5	0	11298.809	.811	<b>1</b>	85.2	14.8	11298.809	.809	0	14.8 85.2
6	0	6	11223.335	.333	-1	99.0	1.0	11223.335	.333	-1	0.7 99.3
6	1	6	11223.336	.333	-2	99.3	0.7	3.1223.336	.333	-2	1.0 99.0
6	1	5	11276.820	.817	-2	<b>91.7</b>	8.3	1.1276.821	.819	-3	4.9 95.1
6	2	5	11276.810	.819	9	95.1.	4.9	1.1.276.81.1	.817	6	8.3 91..7
<b>6</b>	<b>2</b>	<b>4</b>	11320.090	.100	9	97.0	3.0	31320.091			3.0 97.0
6	3	4	1.1319.755	.744	10	96.0	4.0	11319.755	.744	-10	4.0 96.0
6	3	3	11354.265	.269	3	83.0	17.0	1.1354.265	.262	-2	17.0 83.0
6	4	3	11350.244	.243	0	71.6	28.4	1.1350.243	.247	3	28.4 71.6
6	4	2	11384.109	.114	4	58.3	41.7	11384.108			41.7 58.3
<b>6</b>	<b>5</b>	<b>2</b>	13.368.395	.402	7	39.7	60.3	11368.396	.403	7	60.3 39.7
<b>6</b>	<b>5</b>	<b>1</b>	11387.005	.009	3	65.9	34.1	11387.004			34.3 65.9
6	6	1	11416.738			77.4	22.6	11.416.738	.738	0	22.6 77.4
6	6	0	11416.885	.883	-3	80.5	39.5	11416.884			<b>19.5</b> 80.5
7	0	7	11289.949	.949	0	54.4	45.6	11289.948	.949	0	0.5 99.5
7	1	7	11289.949	.949	0	99.5	0.5	11289.94"9	.949	0	45.6 54.4
<b>7</b>	<b>1</b>	<b>6</b>	11353.158	.152	-5	61.7	38.3	11353.157	.152	-4	35.5 84.5

Table 5 (continued)

J	K <sub>a</sub>	K <sub>c</sub>	(311)				(212)						
			E <sub>calc</sub>	E <sub>obs</sub>	O-C	Mixing	E <sub>calc</sub>	E <sub>obs</sub>	O-C	Mixing			
7	2	6	11353.156	.152	-3	84.5	<b>15.5</b>	11353.156	.152	-3	38.3	61.7	
<b>7</b>	<b>2</b>	<b>5</b>	11406.014			<b>92.3</b>	7.7	11406.014			7.3	92.7	
7	3	5	11405.951	.958	6	92.6	7.4	11405.952			7.8	92.2	
7	3	4	11448.766			94.2	5.8	11448.765			5.8	94.2	
7	4	4	11447.621	.610	-10	91.1	8.9	11447.621			8.9	91.1	
7	4	3	11483.626			81.2	18.8	11483.626			18.8	81.2	
7	5	3	11475.351			62.4	37.6	11475.349			37.6	62.4	
7	5	2	11516.747			60.9	39.1	11516.748			39.1	60.9	
7	6	2	11493.798			40.4	59.6	11493.798			59.6	40.4	
7	6	1	11518.215			55.8	44.2	11518.213			44.3	55.7	
7	7	1	3.1554	.719	.720	0	74.6	25.4	11554.718			25.4	74.6
7	7	0	11.554	.772			76.3	23.7	11554.773	.786	1.2	23.7	76.3
8	0	8	11365.350	.350	0	99.7	0.3	11365.351	.350	0	0.3	99.7	
8	1	8	11365.349	.350	0	99.7	0.3	11365.349	.350	0	0.3	99.7	
8	1	7	11438.269	.263	-5	98.8	1.2	11438.268	.263	-4	45.2	54.8	
8	2	7	11438.268	.263	-4	54.8	<b>45.2</b>	11438.268	.263	-4	1.2	98.8	
8	2	6	11500.747			81.1	<b>18.9</b>	11500.747			15.2	84.8	
8	3	6	11500.735	.728	-7	84.8	15.2	11500.736	.728	-8	18.9	81.1	
8	3	5	11552.837			90.3	9.7	11552.838			9.7	90.3	
8	4	5	11552.584			89.9	1.01	11552.584			10.1	89.9	
8	4	4	11595.198			90.4	9.6	11595.197			9.6	90.4	
8	5	4	11592.157			82.9	17.1	11592.157			17.1	82.9	
8	5	3	11617.204			45.7	54.3	11617.203			54.3	45.7	
8	6	3	11669.334			53.5	46.5	11669.333			46.5	53.5	
8	6	2	13668.659			64.0	36.0	11668.660			36.0	64.0	
8	7	2	11638.025			44.1	55.9	11638.026			55.9	44.1	
8	7	1	31631.477			79.1	20.9	11631.478			20.9	79.1	
8	8	1	11712.238			71.7	28.3	11712.238			28.3	71.7	
8	8	0	33712.259			72.6	27.4	11712.259			27.4	72.6	

Table 6. Fitted constants (in  $\text{cm}^{-1}$ ) of local mode pairs of  $\text{H}_2\text{S}$

	(303. ) and (202)	(311)-(212)
$E_v$	9911.0225	11008.6836
A	9.61481 (29)	9.92916(51)
B	8.63533(33)	8.84191(19)
c	4.47661(12)	4.41553(61)
Dk 1000	3.990(16)	4.067(34)
Djk 1000	-2.563(10)	-2.3682(44)
Dj 10000	6.531(32)	6.5609(51)
dk 10000	-3.1.55(67)	-6.0
dj 30000	2.950(10)	2.9705(29)
Hk 1000000	1.8	2.83(53)
Cx z	0.569651(88)	-0.6081.71(87)
Standard deviation	0.006 $\text{cm}^{-1}$	0.005
Number of levels	120	129

Estimated uncertainties are 1 sigma in the last digit.  
 Parameters without uncertainties were held fixed.